Submitted to Nuclear Physics

C.R.N. Strasbourg
CBLL 72-1
Revised Version
4th July 1972

AN ANALYSIS OF THE $K^+\pi^+\pi^-$ SYSTEM PRODUCED IN 10 GeV/c K^+ COHERENT INTERACTIONS ON NUCLEI

A. HAATUFT, A. HALSTEINSLID, K. MYKLEBOST, K. NORDBØ, J.M. OLSEN
University of Bergen

R. ARNOLD, B. ESCOUBES, A. LLORET, M. PATY, J.L. RIESTER, S. de UNAMUNO
Laboratoire de Physique Corpusculaire, Centre de Recherches Nucléaires, Strasbourg

M. HAGUENAUER, W. MICHAEL+, P. MINE, U. NGUYEN-KHAC++
Laboratoire de Physique Nucléaire des Hautes Energies, Ecole Polytechnique, Paris

L. FERRER, P. LADRON DE GUEVARA, R. LLOSA, M. TOMAS
Junta de Energia Nuclear, Madrid

Abstract

The coherent production process K^+-nucleus → $K^+\pi^+\pi^-$ - nucleus has been analysed at 10 GeV/c, in a heavy liquid bubble chamber. Evidence for coherent process is obtained from the momentum transfer distribution ; the cross section is 2.12 ± 0.36 mb per nucleus. The $K^+\pi^+\pi^-$ mass distribution of the coherent events shows abundant production of the so-called Q^+ state, with a cross section of 1.70 ± 0.30 mb per nucleus. A Dalitz plot analysis of the $K^+\pi^+\pi^-$ system indicates $J^P = 1^+$ for the Q^+ with a high probability. The predominant decay is $K^*\pi$ with some contribution of $K\rho$. The density matrix elements for Q^+-production have been studied.

+ *Present address : Lawrence Berkeley Laboratory, California U.S.A.*

++ *Present address : C.E.R.N., Geneva, Switzerland*

1.- INTRODUCTION

We present here a study of the coherent production of the $K^+\pi^+\pi^-$ system by 10 GeV/c K^+ interacting on nuclei.

The experiment has been performed at the C.E.R.N. PS, with the C.E.R.N. Heavy Liquid Bubble Chamber exposed to a radiofrequency separated K^+ beam. The liquid was a propane-freon C_3H_8 - CF_3Br mixture (respectively 60 % and 40 % by volume), of density 0.826g/cm^3 and radiation length X° = 25cm. The magnetic field was about 27 KG.

Previous results from this experiment, on the coherent production of 3, 4 and 5 charged mesons systems [1,2] and on the K^+ neutron charge-exchange process[3], have already been published.

In this paper we report an analysis of the $K^+\pi^+\pi^-$ channel. We first show evidence for the coherent production of this system and give its cross-section. The mass distribution shows an enhancement in the so-called Q-region. Assuming a Q^+ state, we then study its decay by a Dalitz-Plot analysis, and describe some features of its production.

2.- COHERENT PRODUCTION OF THE $K^+\pi^+\pi^-$ SYSTEM

The reaction

$$K^+N \rightarrow K^+\pi^+\pi^- N \qquad (1)$$

(N being a nucleus left unchanged by the reaction) has been looked for in a fiducial region limited to 80cm along the beam direction. The pictures have been scanned to select 3 prongs events with charge +1, without any γ or V° pointing to the interaction, and with no sign of nuclear break-up (for example, identified protons or blobs). A more detailed description of the scanning criteria is given in ref. (2).

A total of about 4300 events have then been measured and submitted to the standard reconstruction programmes ; of these, 2938 were retained after the fitting procedure and the kinematical cut-offs which we now consider.

2 - 1 Kinematical problems

The measured events corresponding to reaction (1) were fitted (1C-fit), the recoil being undetected. The target mass is also unknown ; however, we have verified that, at small momentum transfer, the result of the fit is independent of it. We have therefore used the neutron mass, which corresponds to the effective target at high momentum transfer.

Moreover, there is a (K^+, π^+) ambiguity in the identification of the positive track. This cannot be resolved by the fit, both mass hypotheses having comparable probabilities in almost all the cases. Among the quantities of interest, there is one which does not depend on the (K^+, π^+) assignment, namely the momentum transfer t', usually defined as $t' = |t| - |t|_{min}$. (t is the 4-momentum transfer from the incident K^+ to the final $K^+\pi^+\pi^-$ system, and $|t|_{min}$ is the minimum value allowed for $|t|$). Other quantities, masses for example, do depend on the exact (K^+, π^+) assignment. This ambiguity has been resolved by applying the following selection criteria.

We shall call "T criterion" the following rule : among the two possible assignments for the positive track, the good one is taken as that which gives the smaller $|t|$ value. The efficiency of this criterion has been evaluated using Monte-Carlo generated coherent events distorted by experimental errors. These events were passed through the chain of analysis programmes, and compared to the experimental sample. The effect of the criterion on a given distribution can be estimated by this method, and any biases introduced can be corrected for.

The "T criterion" has been used for the $K\pi\pi$ mass distribution (Fig. 2, see 2-3). For other parameters, for example the branching ratio between the $K^*\pi$ and the $K\rho$ decay modes of the Q^+ (see part 3), a different method has been used. The values of the relevant parameters have been calculated in three different ways : firstly, from a T-selected sample ; then from a sample with a random selection ; and thirdly from an "anti-T selected" sample ("$\bar{T}$-selection", i.e for each event, the wrong hypothesis for T is the good one for $\bar{T}$ and vice-versa). The effect of the experimental resolution on the distributions will be discussed and estimated for each case in the relevant sections.

2 - 2 t' distribution

The experimental t' distribution is given in Fig. 1, for 2285 events with $t' < 0.3$ GeV^2. It has been fitted to a sum of two exponentials, taking as free parameters the two slopes, λ and λ', and their relative contributions ; the fit is remarkably good, having a χ^2 of 5.5 for 11 degrees of freedom, which corresponds to a probability of 92 %. The two exponentials are represented in Fig. 1 by dashed and dotted lines, the first one (high slope) corresponding to the coherent events, the second one (lower slope) to the incoherent part. Whereas the t' distribution is unaffected by the (π^+, K^+) assignment of the positive particle, the result has to be corrected for the experimental resolution and for the background.

The rather poor experimental resolution in heavy liquid induces an important shift in the slope of the exponential. Monte Carlo events generated with various exponential distributions in t', and distorted with our experimental errors, have been analysed as real events. The "true" slope "λ_o" and the "distorted" one "λ" are roughly related by the relation :

$$\lambda^{-1} = \lambda_o^{-1} + \alpha$$

where $\alpha \sim 0.012$ GeV^2 if λ and λ_o are expressed in GeV^{-2}. We have also estimated the background due to spurious reactions :

$$K^+N \rightarrow K^+\pi^+\pi^-\pi^\circ N \qquad (2)$$

$$K^+N \rightarrow K^\circ\pi^+\pi^+\pi^-N \qquad (3)$$

$$K^+ \rightarrow \pi^+\pi^-\pi^+ \text{ (τ decay of the } K^+) \qquad (4),$$

using identified events of these types. It has been estimated that our sample contains about 10 % background (i.e events which satisfy our scanning and fitting criteria), having the same slope as the true incoherent events.

The final values of the slopes of the exponentials - observed and corrected - are given in table I. The value of λ_o (the slope of the coherent differential cross-section) is in agreement with the predictions of the theory of Glauber and Trefil[4] which uses a multiple diffraction formalism to describe the coherent interactions on nuclei at high energies : this model predicts a slope of about 100 GeV^{-2}. The slope of the incoherent part of the spectrum is, on the other hand, in agreement with interactions on free protons, as observed in Hydrogen bubble chambers.

From this result , after background substraction (including that for small t' incoherent events) we obtain the following total cross section[+] for coherent production of the $K^+\pi^+\pi^-$ system :

$$\sigma^{coh}_{nucleus}(K^+\pi^+\pi^-) = 2.12 \pm 0.36 \text{ mb}$$

2 - 3 $K^+\pi^+\pi^-$ mass distribution

A number of experiments on hydrogen targets have been made on the reaction :

$$K^+p \rightarrow K^+\pi^+\pi^-p \qquad (5)$$

[+] In this experiment 1 event corresponds to 0.48 microbarn.

at various energies. The $K^+\pi^+\pi^-$ mass spectra, when the $N^*(1236)$ region for the $p\pi$ effective mass is excluded, show an accumulation of events between 1.15 and 1.45 GeV, the so-called Q^+ bump, with, in some cases, a dip at about 1.3 GeV (between 1.27 and 1.34 GeV, depending on the experiments[5,6]. By performing a general fit to ten experimental results, keeping free the masses, widths and relative amounts of two Breit-Wigner distributions, A. Firestone[7] finds a splitting of the $K^+\pi^+\pi^-$ spectrum into two components : the lower has a mass of 1.250 ± 0.004 GeV, with a width of .182 ± .009 GeV, and the upper a mass of 1.400 ± .006, with a width of .220 ± .014.

In Fig. 2 we present the observed $K^+\pi^+\pi^-$ spectrum in our K^+-nucleus coherent interactions, defined by the following cut-off : $t' < 0.04$ GeV^2. This cut keeps 81 % of the coherent events ; the contribution of incoherent and background events in this region is 30 % of the total number of events. The spectrum shown has been corrected for this contamination by subtracting the normalized distribution of incoherent events, (deduced from events having $t' > 0.06$ GeV; we have verified that the shape of the $K^+\pi^+\pi^-$ mass spectrum for these incoherent events is insensitive to such a t' cut). The (K^+, π^+) ambiguity has been solved by the "T criterion".

A very large fraction of our events is produced with a mass between 1.05 and 1.45 GeV. Taking into account the effect of the form factor of the nucleus, which decreases the production rate by a factor of about 2 when the mass goes from 1.05 to 1.45 GeV, the experimental central value is 1.265 ± .010 GeV. The experimental observed width is about 300 MeV. Fig. 3 shows the Dalitz plot for those events having

$t' < 0.04$ GeV^2, and $1.1 \leqslant M(K^+\pi^+\pi^-) \leqslant 1.4$ GeV. The projection on the $K^+\pi^-$ mass axis shows an important production of K^*_{890} events, with a mean value for the mass of 0.892 GeV. The experimental observed width is about 110 MeV.

We conclude that our $K^+\pi^+\pi^-$ mass spectrum has a ratio of signal/background for the Q^+ bump larger than that observed in hydrogen experiments[5] (which have no t' cut). A more detailed study of coherent production in the Q-region is in progress. In particular the effects of the experimental resolution and of the momentum transfer cut are being studied in order to make a precise comparison with the Q-mass and width values obtained in recent hydrogen experiments.

2 - 4 Coherent production cross-section

To obtain the cross section of Q^+ coherent production, we keep the events defined by $1.05 \leqslant M(K^+\pi^+\pi^-) \leqslant 1.45$ GeV, and $t' < 0.04$ GeV^2 ; we correct for the coherent events lost by the t' cut and for the incoherent events and background contamination in the small t' region. The result is

$$\sigma^{coh}_{nucleus}(Q^+ \to K^+\pi^+\pi^-) = 1.70 \pm 0.30 \text{ mb}$$

3.- DECAY AND PRODUCTION OF THE Q^+-STATE

Having shown evidence for abundant Q^+ production, we now study its production and decay properties.

3 - 1 Parametrization of the Dalitz plot density

The Q^+ decay properties have been extensively studied in K^+p interactions[8]. Spin-parity analysis favours a 1^+ state, and the decay modes are $K^*\pi$ and $K\rho$. The present experiment offers the possibility of analyzing the decay properties of the Q^+ enhancement found in K^+-nucleus diffraction dissociation.

We can test all the possible spin-parity assignations for the Q^+ up to $J = 2$, taking as the decay modes :

$$Q^+ \to K^+\rho^\circ \quad , \quad \rho^\circ \to \pi^+\pi^- \qquad (6)$$

$$Q^+ \to K^{*\circ}\pi^+ \quad , \quad K^{*\circ} \to K^+\pi^- \qquad (7)$$

$$Q^+ \to K^+\pi^+\pi^- \quad , \quad \text{direct mode} \qquad (8)$$

The two-step decays (6) and (7) via a vector meson (ρ° or K^*) can be described by using the phenomenological tensor coupling approach[9]. For each spin-parity hypothesis of the Q^+, we make a parametrization which depends only on the ratio between the coupling constants for both modes.

In fact we must consider the spin-parity of the Q^+-state. If the Q^+ belongs to the natural series ($P_Q = (-1)^J Q$), the orbital angular momentum L between the intermediate vector meson and the pseudoscalar meson can take only the value $L = J$. If the Q^+ belongs to the unnatural series ($P_Q = (-1)^{J Q + 1}$), one has $L = J \pm 1$, except when $J = 0$. We have neglected, in the case of "unnatural Q^+", the possible interference between the $L = J-1$ and $L = J+1$ partial waves.

For the parametrization of the Dalitz plot density in the Q-center of mass system, the following notation[10] is used :

- the three pseudo-scalar mesons are referred to index i : $i = 1 : K^+$, $i = 2 : \pi^+$, $i = 3 : \pi^-$, with 4-momenta in the final state : $P_i\ (E_i, P_i)$

- the two vector mesons are denoted by $V_1=(2,3)=\rho$, $V_2 = (3,1) = K^*$, their squared invariant masses being $V_i = (P_j + P_K)^2$

- the effective mass of the 3 mesons system is $m_Q = E_1 + E_2 + E_3$.

One has

$$\mathscr{D}_L^{J^P}(E_1, E_2, m_Q ; Z_1, Z_2, Z_3) = \frac{1}{m_Q}\left\{ \sum_{m=-J}^{+J} \left| Z_1 F_M^J [1,23] + Z_2 F_M^J [2,31] + Z_3 \right|^2 \right\} \quad (9)$$

where z_1, z_2, z_3 are proportional to the coupling constants of the three processes (6), (7) and (8). $F^J_{M,L}(i,k)$ is the invariant transition amplitude between a pure JM > state and a final state of orbital momentum L between the pseudoscalar meson i and the vector meson $V_i(j,k)$.

The propagator of the vector meson V_j is

$$P_j = \frac{\sqrt{\frac{M_j \Gamma_j}{\pi}}}{(S_j - M_j^2) + i M_j \Gamma_j} \quad (10)$$

M_j and Γ_j being the mass and width of V_j.

The amplitude $F^J_{M,L}(i,k)$ is written as a sum over the polarizations λ of the V_j vector meson :

$$F_M^J [i,jk] = P_i \sum_n R^J_{M,n}(Q \to V_i P_i) . S_n(V_i \to P_j P_k) \quad (11)$$

The two matrix elements R and S are obtained from the contraction of the simplest tensors which can describe the kinematics of the two steps of the Q decay.

After summing up over all the final state polarizations, one gets :

$$\frac{d^3\sigma}{dE_1 dE_2 dm_Q} \sim \mathscr{D}_L^{J^P}(E_1, E_2, m_Q ; \alpha\ \phi\ b) = \frac{1}{m_Q}\Big\{ \sin^2\alpha |P_1|^2\ A^{J^P}(1,1) + 2\sin\alpha\cos\alpha\ \mathrm{Re}\left(P_1 P_2\ e^{i\phi}\right) A^{J^P}(1,2) + \cos^2\alpha |P_2|^2\ A^{J^P}(2,2) + b\Big\} \tag{12}$$

where the quantities $A_L^J(i,\ell)$ are given by :

$$A^{J^P}(i,\ell) = \sum_{M=-J}^{+J} \left(\sum_p R_{M,p}^{J^P}(Q \to V_i P_i).S_p(V_i \to p_j p_k) \right) \left(\sum_q R_{M,q}^{*J^P}(Q \to V_\ell P_\ell).\ S_q^*(V_\ell \to p_m p_n) \right) \tag{13}$$

Table II gives the dependance of $A_L^J(i,\ell)$ on the 4-momenta P_i of the 3 final particles.

We have introduced three free parameters, α, ϕ and b. α and ϕ express the ratio between the coupling constants z_1 and z_2 of the $K\rho$ and $K^*\pi$ decays :

$$\frac{z_1}{z_2} = \mathrm{tg}\alpha\ e^{i\phi}, \tag{14}$$

where $0 \leqslant \alpha \leqslant \pi/2$; $\alpha = 0$ corresponds to a pure $K^*\pi$ decay, $\alpha = \pi/2$ to a pure $K\rho$ decay. The angle ϕ is such that $0 \leqslant \phi \leqslant 2\pi$, and the value $\phi = 0\ (\pi)$ corresponds to a completely destructive (constructive) interference between the two decay modes.

The third parameter b is related to the proportion of the direct process (8) plus the background : b is real and > 0.

3 - 2 Fitting procedure and results

The coherently produced Q^+ events are defined by $1.1 < M_Q < 1.4$ GeV, $t' \leq 0.04$ $(GeV/c)^2$; 684 events remain after these cut-offs with a background from incoherent event of 20 %. Fig. 3 shows the Dalitz plot for these events. The boundary corresponds to the upper limit taken for the Q mass. The curves on the projected distributions are i) phase - space prediction, ii) the result of the fit on the Dalitz plot density assuming that the Q^+ is in a $J^P(L) = 1^+(S)$ state. (see below).

The maximum likelihood function for each $J^P(L)$ hypothesis is given by

$$\mathcal{L}(\alpha,\phi,b) = \prod_{i=1}^{N} p^{J^P}(E_1^i, E_2^i, m_Q^i \; ; \; \alpha \; \phi \; b) \qquad (16)$$

$$p^{J^P}(E_1^i, E_2^i, m_Q^i \; ; \; \alpha \; \phi \; b) = \frac{\mathcal{D}^{J^P}(E_1^i, E_2^i, m_Q^i \; ; \; \alpha \; \phi \; b)}{\int_{m_Q^i} dE_1 \, dE_2 \, \mathcal{D}^{J^P}(E_1, E_2, m_Q^i ; \alpha \; \phi \; b)}$$

$\mathcal{D}$ is given by (11) ; the integration in the denominator is made over all the values of E_1 and E_2 which are compatible with the fixed value of the three-meson invariant mass m_Q^i for a given bin i.) The fitting procedure used[11] minimizes $M(\underset{\sim}{X}) = -\mathrm{Log}\mathcal{L}$ as a function of the three parameters $X_1 = \alpha$, $X_2 = \phi$, $X_3 = b$. The goodness of the fit is obtained by comparing the χ^2 of the experimental and theoretical Dalitz plots, the theoretical plot being calculated by taking the fitted parameters as input for a Monte-Carlo generation programme[12]. The masses and widths of the ρ and the K^* have been taken as follows :

$$\rho : M_1 = 760 \ , \quad \Gamma_1 = 150 \text{ MeV}$$
$$K^*: M_2 = 892 \ , \quad \Gamma_2 = 100 \text{ MeV}$$

The results are given in Table III. The best fit is obtained for the $1^+(S)$ hypothesis, with a $\chi^2/N = 0.67$, corresponding to a 93,2 % probability ; the $2^-(P)$ hypothesis has a $\chi^2/N = 1.5$, corresponding to a 4 % probability. All the other hypotheses are ruled out.

Fig. 4 shows the results of the fits on the Dalitz plot projections $M(K^+\pi^-)$ and $M(\pi^+\pi^-)$. The agreement with the $1^+(S)$ hypothesis is excellent.

We have also tried to estimate the relative contributions of each wave inside the unnatural spin-parity series ; for this, we have written the Dalitz plot density as a linear combination of the five pure states densities from this series. Let us denote as $j = 1,2,3,4,5$ the states, respectively $0^-(P)$, $1^+(S)$, $1^+(D)$, $2^-(P)$, $2^-(F)$. The new likelihood function is :

$$\mathscr{L}(\alpha_1\phi_1\xi_1,\ldots\alpha_5\xi_5;b) = \prod_{i=1}^{N} \frac{\sum_{j=1}^{5} \xi_j \mathscr{D}^j(E_1^i, E_2^i, m_Q^i \ ; \ \alpha_j\phi_j) + b/m_Q^i}{\int_{m_Q^i} dE_1 \, dE_2 \left[\sum_{j=1}^{5} \xi_j \mathscr{D}^j(E_1, E_2, m_Q^i; \alpha_j\phi_j) + b/m_Q^i\right]} \qquad (17)$$

where ξ_j stands for the proportion of the j state. With the constraint $(\sum_{j=1}^{5} \xi_j) + b = 1$ there are 15 independant parameters. The function $\mathscr{D}^j$ is defined by :

$$\mathscr{D}^j(E_1, E_2, m_Q^i; \alpha_j\phi_j) = \frac{1}{m_Q^i}\Big[\sin^2\alpha_j |P_1|^2 \, A^j(1,1) + 2\sin\alpha_j \cos\alpha_j \, \mathrm{Re}\left(P_1 P_2^* e^{i\phi}\right) A^j(1,2)$$
$$+ \cos^2\alpha_j |P_2|^2 \, A^j(2,2)\Big] \qquad (18)$$

The results are given in table IV. Here again the most important contribution comes from the $1^+(S)$ wave, followed by $0^-(P)$. However, due to the high number of parameters for a limited statistics, this result is less reliable than the preceding one. The errors on the fitted parameters are very large, except for the $1^+(S)$ state.

The values of the parameters α^*, ϕ^* and b^* which minimize $-\text{Log}\mathcal{L}$, are given in table III. As they have been calculated using the T-criterion, one has to correct for the fact that the wrong assignment is made in 25 % of the cases. After applying this correction, we obtain, for the $1^+(S)$ hypothesis :

i) for the ratio of the amplitudes : $\text{tg}\alpha = \frac{Q \to K\rho}{Q \to K^*\pi}$, the value $\alpha = 0.47 \pm 0.07$ radian.

ii) for the phase between the two amplitudes : $\pi \leqslant \phi \leqslant \frac{3\pi}{2}$.

These values correspond to the following results for ($Q \to K^*\pi$ / $Q \to K\rho$ / interference between these modes / direct $K^+\pi^+\pi^-$ + background) respectively :

$$(60 \pm 8)\% \quad / \quad (13 \pm 2)\% \quad / \quad (14 \pm 2)\% \quad / \quad (13 \pm 4)\%$$

These results are in good agreement with a similar experiment done on Q^- coherent production by K^- on nuclei at the same energy[13], which gives for the parameters :

$$\alpha = 0.42 \pm 0.08 \qquad \phi = 3.18 \pm 0.21$$

and for the branching ratios :

$$(65 \pm 5)\% \quad / \quad (11.5 \pm 4)\% \; / \; (9.5 \pm 3.5)\% \; / \; (14 \pm 7)\%.$$

Our estimation of the phase ϕ is however less precise.

Other evidence for the $1^+(S)$ dominance in the Q^+ decay comes from the angular distribution of the K^* in the Q center of mass system. The polar and azimuthal angle distributions are given in Fig. 5 for events defined as $Q^+ \to K^*\pi^+$, i.e. having a $K^+\pi^-$ mass combination in the K^*: $0.830 \leq M(K^+\pi^-) \leq 0.950$ GeV. Both distributions are compatible with isotropy, which indicates a s-wave between the K^* and the π^+. For these $K^*\pi$ events, Fig. 6 shows the distribution of the cosine of the angle between the two pions (π^+ and π^-) in the K^* center of mass system. There is some asymetry favouring the emission of the two pions in opposite directions, which is just what is expected from the $1^+(S)$ hypothesis for the $Q \to K^*\pi$. The solid curve on Fig. 6 is obtained from the Dalitz plot density fit for this hypothesis.

3 - 3 Q^+ production properties

Knowing that the Q^+ is in a definite state ($1^+(S)$), we can study the density matrix element by considering the experimental angular distribution of the normal to the Q decay plane. The theoretical distribution, calculated by Jackson[14], is :

$$\frac{dN}{d\alpha\, d\cos\beta} = \rho_{oo}\sin^2\beta + \rho_{11}(1+\cos^2\beta) + \rho_{1,-1}\sin^2\beta\cos 2\alpha + \sqrt{2}(\mathrm{Re}\,\rho_{10})\sin 2\beta\cos\alpha - a(1^+)\left[2\sqrt{2}(\mathrm{Im}\,\rho_{10})\sin\beta\sin\alpha\right] \quad (19)$$

where α and β are the azimuthal and polar angles of the normal in the Q center of mass system, referred to a given frame. Berman and Jacob have shown[15] that the term $a(1^+)$ can be neglected. In this experiment, at very small t', the Gottfried-Jackson (T) and helicity (S) systems are practically in coincidence. (S is such that the O_Z axis is parallel to the Q^+ direction, i.e. the T system). Fig. 7 shows the experimental distributions of $\cos\beta$ and α in the T or S

system. Results for fitted density matrix elements in the S and T systems are given in Table V.

These values are compatible with the results of other experiments[16] ; they are in general somethat lower, especially $\rho_{\delta\delta}$, and are affected by larger errors, which come mainly from the (K^+, π^+) ambiguity.

Other features of the Q^+ production are found in the $K^*\pi$ events, defined as above. We have looked at the distribution of the alignment angle of the outgoing K^+ in the K^* center of mass system (Fig. 8). An asymmetry can be observed, which favours forward emission of the outgoing K^+, i.e. in the same direction as the incident particle. This feature has been already observed in other experiments[8].

C O N C L U S I O N

We clearly observe the Q^+ enhancement in the study of the $K^+\pi^+\pi^-$ system, produced coherently in 10 GeV/c K^+ interactions on nuclei. The Q^+ coherent production cross section is equal to 1.70 ± 0.30 mb.

The Dalitz plot analysis gives a spin-parity assignement of $J^P = 1^+$ for the Q^+ ; the dominant decay modes are $K^*\pi$ and $K\rho$ in an s-wave.

Acknowledgments

We wish to thank Professors LEPRINCE-RINGUET, A. ROUSSET, B. TRUMPY, P. CÜER, J.M. OTERO NAVASCUES and C. SANCHEZ DEL RIO for their support and encouragements. We are indebted to the operation crews of the C.E.R.N. proton synchrotron and the C.E.R.N. Heavy Liquid Bubble Chamber.

Table Captions

Table I : Coherent and incoherent events. Observed and corrected slopes.

Table II : Kinematical dependance of the $A_L^J(i,1)$ (see formula (13)).

Table III : Results of fitting the Dalitz plot density to each spin-parity hypothesis separately.

Table IV : Results of fitting simultaneously the Dalitz plot density to the five lowest spin-parity hypotheses of the unnatural series.

Table V : Fitted density matrix elements in the S and T systems.

Figure Captions

Figure 1 : t' distribution for 2285 events ($t' < 0.3$ GeV^2)

Figure 2 : $K^+\pi^+\pi^-$ mass spectrum for the coherent events with $t' < 0.04$ GeV^2. Incoherent and background events have been subtracted.

Figure 3 : Dalitz plot for the Q^+ events with $1.1 < M(K^+\pi^+\pi^-) < 1.4$ GeV and $t' < 0.04$ GeV^2

Figure 4 : Fits to the Dalitz plot projections for the different hypotheses of the natural serie (A) and the unnatural serie (B)

Figure 5 : Polar (a) and azimuthal (b) emission angles of the K^* in the Q^+ center of mass system of the $Q^+ \to K^*\pi$ events. A pure $1^+(S)$ state would give isotropic distributions

Figure 6 : Distribution of the cosine of the angle between π^+ and π^- evaluated in the K^* center of mass system, for the $Q^+ \to K^*\pi$ events. The curve corresponds to the fit to the Dalitz plot density for the $1^+(S)$ hypothesis

Figure 7 : Polar (a) and azimuthal (b) distributions of the direction of the normal to the Q^+ decay plane. The angles are evaluated for the T frame in the Q^+ center of mass system. The curve corresponds to the $1^+(S)$ fitted distribution (see formula (19)).

Figure 8 : Alignment (a) and azimuthal (b) angles for the K^* ($Q^+ \to K^*\pi^+$ events) in the K^* center of mass system

R E F E R E N C E S

(1) M. HAGUENAUER, W. MICHAEL, P. MINE, U. NGUYEN-KHAC, A. HAATUFT, A. HALSTEINSLID, K. MYKLEBOST, K. NORDBØ, J.M. OLSEN, H. ANNONI, R. ARNOLD, A. LLORET, M. PATY, J.L. RIESTER, B. ESCOUBES, L. FERRER, P. LADRON de GUEVARA, R. LLOSA and S. de UNAMUNO
Physics Letters 34B (1971) 219

(2) B. ESCOUBES
Thèse - Université de Paris-Sud (ORSAY, 1971)

(3) M. HAGUENAUER, P. MINE, U. NGUYEN-KHAC, K. BJØRNENAK, A. HAATUFT, J.M. OLSEN, R. ARNOLD, B. ESCOUBES, A. LLORET, M. PATY, J.L. RIESTER, S. de UNAMUNO, L. FERRER, P. LADRON de GUEVARA and R. LLOSA
Physics Letters 37B (1971) 538

(4) R. J. GLAUBER, in "High Energy Physics and Nuclear Structure", edited by G. ALEXANDER (North Holland Amsterdam, 1967), 311
J.S. TREFIL, Phys. Rev. 180, (1969) 1366

(5) At 4.3 GeV/c :

B. FORMAN, N.M. GELFAND, P. LEARY, F. MOSER, A. SEIDL and J. WOLFSON
Phys. Rev. D3 (1971) 2610

At 4.6 GeV/c :

B.C. SHEN, I. BUTTERWORTH, C. FU, G. GOLDHABER, S. GOLDHABER and G.H. TRILLING
Phys. Rev. Letters 17 (1966) 726

At 5.0 GeV/c :

G. BASSOMPIERRE, Y. GOLDSCHMIDT-CLERMONT, A. GRANT, V.P. HENRI, I. HUGHES, B. JONGEJANS, R.L. LANDER, D. LINGLIN, F. MULLER, J.M. PERREAU, I. SAITOV, R.L. SEKULIN, G. WOLF, W. DE BAERE, J. DEBAISIEUX, P. DUFOUR, F. GRARD, J. HEUGHEBAERT, L. PAPE, P. PEETERS, F. VERBEURE, R. WINDMOLDERS, M. JOBES and W. MATT
Phys. Letters 26B (1967) 30

At 5.5 GeV/c :

F. BOMSE, S. BORENSTEIN, A. CALLAHAN, J. COLE, B. COX, D. ELLIS, L. ETTLINGER, D. GILLESPIE, G. LUSTE, R. MERCER, E. MOSES, A. PEVSNER and R. ZDANIS
Phys. Rev. Letters 20 (1968) 1519

At 7.3 GeV/c :

C.Y. CHIEN, P.M. DAUBER, E.I. MALAMUD, D.J. MELLEMA, P.E. SCHLEIN, P.A. SCHREINER, W.E. SLATER, D.H. STORK, H.K. TICHO and T.G. TRIPPE
Phys. Letters 28B (1968) 143

At 9.0 GeV/c :

G. ALEXANDER, A. FIRESTONE, G. GOLDHABER and D. LISSAUER
Nucl. Phys. B13 (1969) 503

At 10.0 GeV/c :

K.W.J. BARNHAM, D.C. COLLEY, W.P. DODD, S. HUQ, M. JOBES, G.M. JONES, K. PATHAK, L. RIDDIFORD, P. WATKINS, I. GRIFFITHS, I.S. HUGUES, I. McLAREN, C.D. PROCTER, R.M. TURNBULL, I.R. WHITE, B. ALPER, M.G. BOWLER, R.J. CASHMORE, R.J. HEMINGWAY, A.W. LOWMAN and D.J. SUMNER
Nucl. Phys. B25 (1970) 49

At 12.0 GeV/c :

A. BARBARO-GALTIERI, P.J. DAVIS, S.M. FLATTE, J.H. FRIEDMANN, M.A. GARNJOST, G.R. LYNCH, M.J. MATISON, M.S. RABIN, F.T. SOLMITZ, N.M. UYEDA, V. WALUCH and R. WINDMOLDERS,
Phys. Rev. Letters 22 (1969) 1207

At 12.7 GeV/c :

M.S. FARBER, T. FERBEL, P.F. SLATTERY and H. YUTA
Phys. Rev. D1 (1970) 78

(6) At 9.0 GeV/c :

A.F. GARFINKEL, R.F. HOLLAND, D.D. CARMONY, H.W. CLOPP, D. CORDS, F.J. LOEFFLER, L.K. RANGAN, R.L. LANDER, D.E. PELLETT and P.M. YAGER
Phys. Rev. Letters 26 (1971) 1505

(7) A. FIRESTONE, in "Experimental Meson Spectroscopy" edited by C. BALTAY and A.H. ROSENFELD (Columbia University PRESS, New-York 1970) p. 229

(8) See the reference (5), at 7.3, 9.0, 10.0 and 12.7 GeV/c

(9) W.R. FRAZER, J.R. FULCO, F.R. HALPERN
Phys. Rev. 136B (1964) 1207

D. GRIFFITHS, Wayne State University preprint (1968)
and Nucl. Physics, B18 (1970) 24

(10) D. FOURNIER,
Thèse (Université de Paris-Sud, ORSAY, 1970) L.A.L. 1242

(11) F. JAMES and M. ROSS, MINUIT, CERN program library D05
D 506 ; M. ABRAMOVICH, H. BLUMENFELD, F. BRUYANT,
V. CHALOUPKA, S.U. CHUNG, J. DIAZ, L. MONTANET,
S. REUCROFT, J. A. RUBIO, Nucl. Phys. B23 (1970) 467

(12) F. JAMES, FOWL, CERN program Library W 505

(13) B. DAUGERAS, D. FOURNIER, J. HENNESSY, J.J. VEILLET,
A.M. CNOPS, F.R. HUSON, R.I. LOUTTIT, D.J. MILLER,
H.H. BINGHAM, C.W. FARWELL, W.B. FRETTER, G.M. IRWIN,
S. KAHN, A. LU, M. DI CORATO, M. ROLLIER, C. BOUTHET,
J. CRUSSARD and J. GINESTET, Amsterdam International
Conf. on Elementary Particles, Amsterdam 1971,
paper n° 358

(14) J.D. JACKSON in "High Energy Physics" Les Houches Summer
School of Theoretical Physics 1965 (GORDON and BREACH
editors) p. 325

(15) S.M. BERMAN and M. JACOB
Phys. Rev. 139B, (1965), 1023

(16) F. GRARD, P. HERQUET, R. WINDMOLDERS, H.H. BINGHAM,
L. EISENSTEIN, Y. GOLDSCHMIDT-CLERMONT, V.P. HENRI,
J. QUINQUARD, CERN report, CERN/D.Ph. II/PHYS 71-3

TABLE I – Coherent and incoherent events. Observed and corrected slopes.

TYPE	NUMBER OF EVENTS	SLOPES (GeV^{-2})	
		OBSERVED(λ)	CORRECTED(λ_o)
Coherent	1020 ± 118	41.6 ± 4.7	83^{+25}_{-13}
Incoherent + background	1265 ± 118	7.38 ± 0.94	9 ± 1

TABLE II – Kinematical dependance of the $A_L^J(i,1)$ (see formula (13)).

Serie	J^P	L	A(i,j) in the 0 center of mass ($m_2 = m_3$)
NATURAL	0^+	–	Interdit
	1^-	1	$A(1,1) = 4m_Q^2\left[p_1^2 p_2^2 - (\vec{p}_1\cdot\vec{p}_2)^2\right]$ $A(1,2) = A(1,1)$ $A(2,2) = A(1,1)$
	2^+	2	$A(1,1) = 2m_Q^2 p_1^2\left[p_1^2 p_2^2 - (\vec{p}_1\cdot\vec{p}_2)^2\right]$ $A(1,2) = 2m_Q^2(\vec{p}_1\cdot\vec{p}_2)\left[p_1^2 p_2^2 - (\vec{p}_1\cdot\vec{p}_2)^2\right]$ $A(2,2) = 2m_Q^2 p_2^2\left[p_1^2 p_2^2 - (\vec{p}_1\cdot\vec{p}_2)^2\right]$
UNNATURAL	0^-	1	$A(1,1) = m_Q^2(E_3 - E_2)^2$ $A(1,2) = -m_Q^2\left[(E_3 - E_1) + \frac{m_1^2 - m_3^2}{s_2}(E_3 + E_1)\right]\left[E_3 - E_2\right]$ $A(2,2) = m_Q^2\left[(E_3 - E_1) + \frac{m_1^2 - m_3^2}{s_2}(E_3 + E_1)\right]^2$
	1^+	0	$A(1,1) = p_1^2(1+\alpha_1^-)^2 + \vec{p}_1\cdot\vec{p}_2(1+\alpha_1^-) + 4p_2^2$ $A(1,2) = -2p_1^2(1+\alpha_1^-) - 2p_2^2(1+\alpha_2^-) - \vec{p}_1\cdot\vec{p}_2\left[4 + (1+\alpha_1^-)(1+\alpha_2^-)\right]$ $A(2,2) = p_2^2(1+\alpha_2^-)^2 + \vec{p}_1\cdot\vec{p}_2(1+\alpha_2^-) + 4p_1^2$
		2	$A(1,1) = m_Q^2 p_1^4\left[p_1^2(1+\alpha_1^+)^2 + \vec{p}_1\cdot\vec{p}_2(1+\alpha_1^+) + 4p_2^2\right]$ $A(1,2) = m_Q^2 p_1^2 p_2^2\left\{-2p_1^2(1+\alpha_1^+) - 2p_2^2(1+\alpha_2^+) - \vec{p}_1\cdot\vec{p}_2\left[4 + (1+\alpha_1^+)(1+\alpha_2^+)\right]\right\}$ $A(2,2) = m_Q^2 p_2^4\left[p_2^2(1+\alpha_2^+)^2 + \vec{p}_1\cdot\vec{p}_2(1+\alpha_2^+) + 4p_1^2\right]$
	2^-	1	$A(1,1) = \left[p_1^2(1+\beta_1^-) + 2\vec{p}_1\cdot\vec{p}_2\right]^2 + 3\left[p_1^2 p_2^2 - (\vec{p}_1\cdot\vec{p}_2)^2\right]$ $A(1,2) = 2\vec{p}_1\cdot\vec{p}_2\left[p_1^2(1+\beta_1^-) + p_2^2(1+\beta_2^-)\right] + (\vec{p}_1\cdot\vec{p}_2)^2\left[1 + \frac{3}{2}(1+\beta_1^-)(1+\beta_2^-)\right] + 3p_1^2 p_2^2\left[1 - \frac{1}{6}(1+\beta_1^-)(1+\beta_2^-)\right]$ $A(2,2) = \left[p_2^2(1+\beta_2^-) + 2\vec{p}_1\cdot\vec{p}_2\right]^2 + 3\left[p_1^2 p_2^2 - (\vec{p}_1\cdot\vec{p}_2)^2\right]$
		3	$A(1,1) = m_Q^2 p_1^4\left[p_1^2(1+\beta_1^+) + 2\vec{p}_1\cdot\vec{p}_2\right]^2 + 3\left[p_1^2 p_2^2 - (\vec{p}_1\cdot\vec{p}_2)^2\right]$ $A(1,2) = m_Q^2 p_1^2 p_2^2\left\{2\vec{p}_1\cdot\vec{p}_2\left[p_1^2(1+\beta_1^+) + p_2^2(1+\beta_2^+)\right] + (\vec{p}_1\cdot\vec{p}_2)^2\left[1 + \frac{3}{2}(1+\beta_1^+)(1+\beta_2^+)\right] + 3p_1^2 p_2^2\left[1 - \frac{1}{6}(1+\beta_1^+)(1+\beta_2^+)\right]\right\}$ $A(2,2) = m_Q^2 p_2^4\left[p_2^2(1+\beta_2^+) + 2\vec{p}_1\cdot\vec{p}_2\right]^2 + 3\left[p_1^2 p_2^2 - (\vec{p}_1\cdot\vec{p}_2)^2\right]$

$$\alpha_1^{\pm} = -(E_3 - E_2)\,\frac{{}^{\pm}{}_{-1}^{2}a_1}{{}^{\pm}{}_{-1}^{1}a_1}\,m_Q \qquad S_2 = m_Q^2 + m_2^2 - 2m_Q E_2$$

$$\beta_1^{\pm} = -(E_3 - E_2)\,\frac{{}^{\pm}{}_{-1}^{2}a_1}{{}^{\pm}{}_{-1}^{2}a_1}\,m_Q\,p_1^2$$

$$\alpha_2^{\pm} = \frac{m_1^2 - m_3^2}{s_2} - \left[(E_3 - E_1) + \frac{m_1^2 - m_3^2}{s_2}(E_3 + E_1)\right]\frac{{}^{\pm}{}_{-1}^{2}a_2}{{}^{\pm}{}_{-1}^{1}a_2}\,m_Q$$

$$\beta_2^{\pm} = \frac{m_1^2 - m_3^2}{s_2} - \left[(E_3 - E_1) + \frac{m_1^2 - m_3^2}{s_2}(E_3 + E_1)\right]\frac{{}^{\pm}{}_{-1}^{2}a_2}{{}^{\pm}{}_{-1}^{2}a_2}\,m_Q\,p_2^2$$

TABLE III - Results of fitting the Dalitz plot density to each spin-parity hypothesis separately.

	$J^P(L)$ HYPOTHESIS						
	1^- P	2^+ D	0^- P	1^+ S	1^+ D	2^- P	2^- F
$M(\vec{X}^*)$	2026	2033	2061	1915	2042	1958	2052
χ^2(33 d.o.f.)	103	90	106	22	100	48	107
α^*	0,82	0,81	0,24	0,57	0,39	0,61	0,68
$\Delta\alpha^*$	0,14	0,04	0,08	0,06	0,08	0,07	0,05
φ^*	1,44	6,28	4,37	3,95	1,64	1,39	1,87
$\Delta\varphi^*$	0,17	0,11	0,40	0,16	0,49	0,26	0,20
b^*	0,024	0,000	0,043	0,068	0,005	0,004	0,000
Δb^*	0,006	0,008	0,007	0,020	0,001	0,001	0,000

TABLE IV – Results of fitting simultaneously the Dalitz plot density to the five lowest spin-parity hypotheses of the unnatural series.

	$J^P(L)$ HYPOTHESIS				
	0^- P	1^+ S	1^+ D	2^- P	2^- F
Proportion of each hypothesis	0,31 ± 0,12	0,63 ± 0,18	0,005 ± 0,002	0,004 ± 0,001	0,009 ± 0,003
α^*	0,29	0,59	0,52	0,09	1,50
$\Delta\alpha^*$	0,68	0,05	1,22	1,02	2,36
φ^*	1,68	4,04	3,92	0,58	5,23
$\Delta\varphi^*$	2,73	0,15	2,68	1,81	6,28

The proportion of the background is : 0,042 ± 0,011

TABLE V - Fitted density matrix elements in the S and T system.

	S SYSTEM	T SYSTEM
ρ_{00}	0,69 ± 0,20	0,70 ± 0,20
ρ_{11}	0,15 ± 0,10	0,15 ± 0,10
ρ_{1-1}	-0,05 ± 0,08	-0,05 ± 0,10
Re ρ_{10}	0,04 ± 0,03	-0,04 ± 0,07

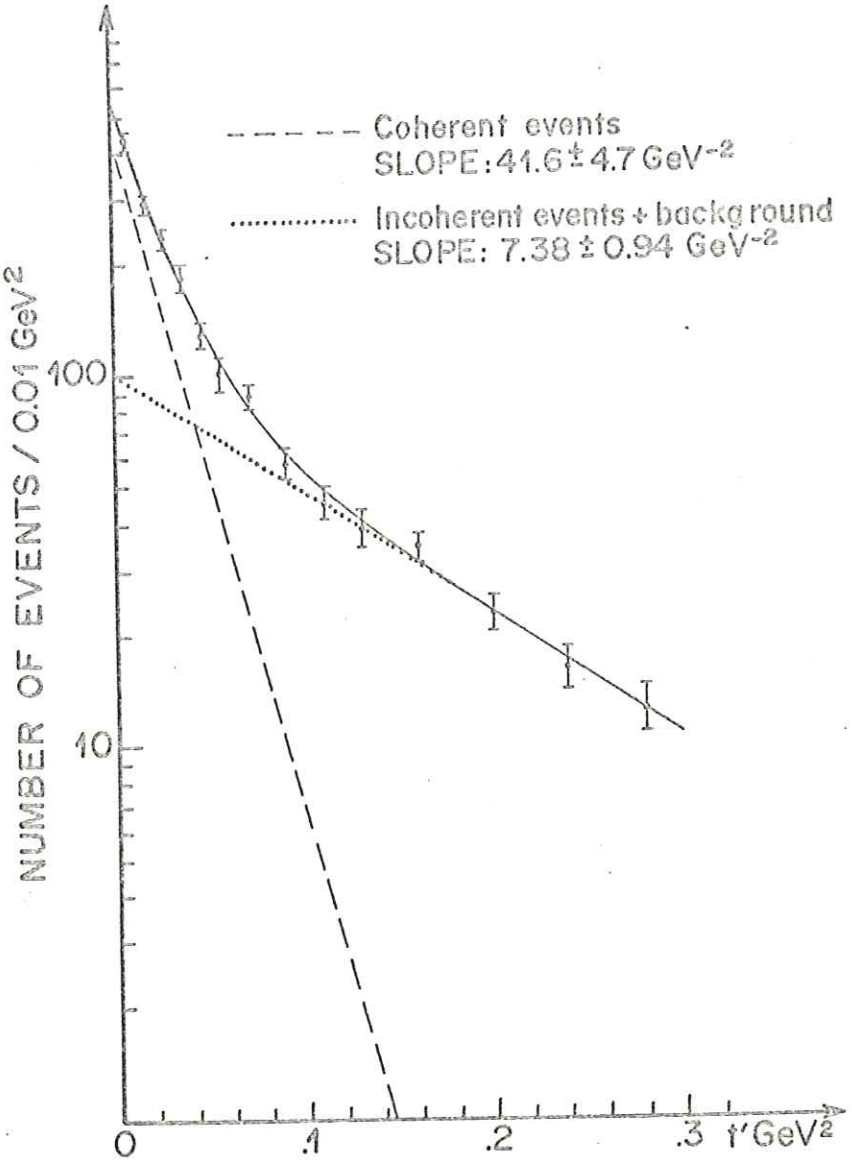

Fig. 1 : t' distribution for 2285 events ($t' < 0.3$ GeV^2)

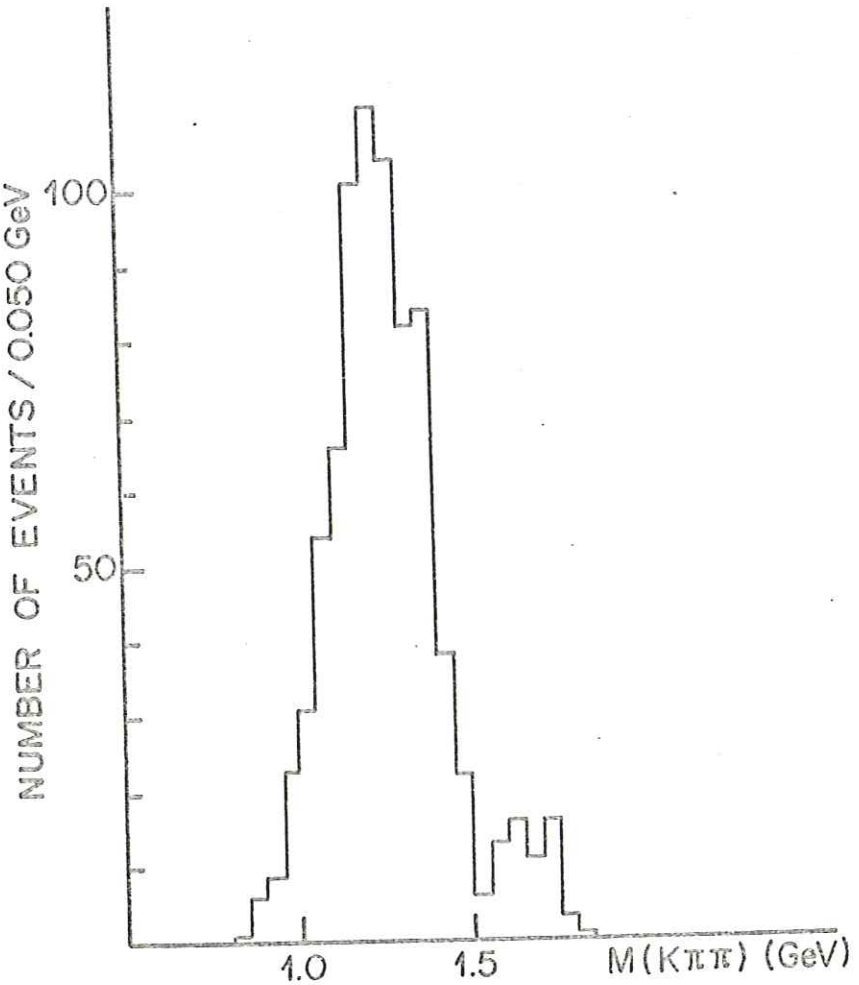

Fig. 2 : $K^+\pi^+\pi^-$ mass spectrum for the coherent events with $t' < 0.04$ GeV^2. Incoherent and background events have been subtracted.

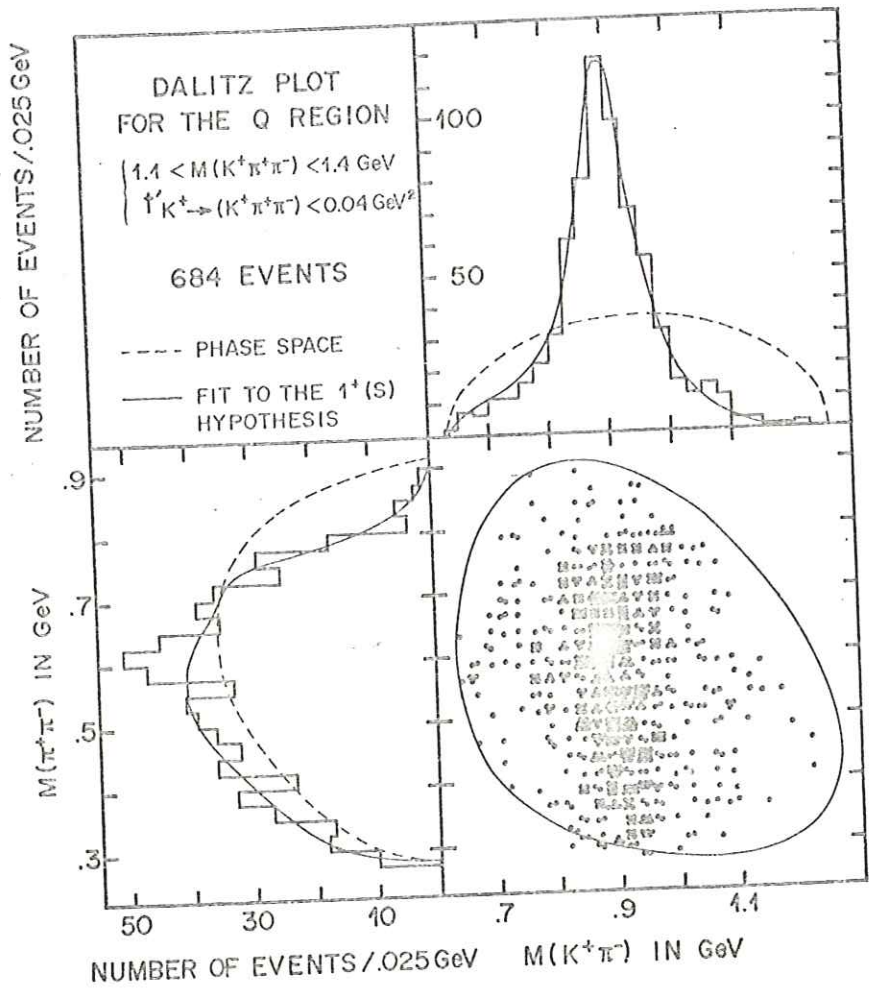

Fig. 3 : Dalitz plot for the Q^+ events with $1.1 < M(K^+\pi^+\pi^-) < 1.4$ GeV and $t' < 0.04$ GeV^2

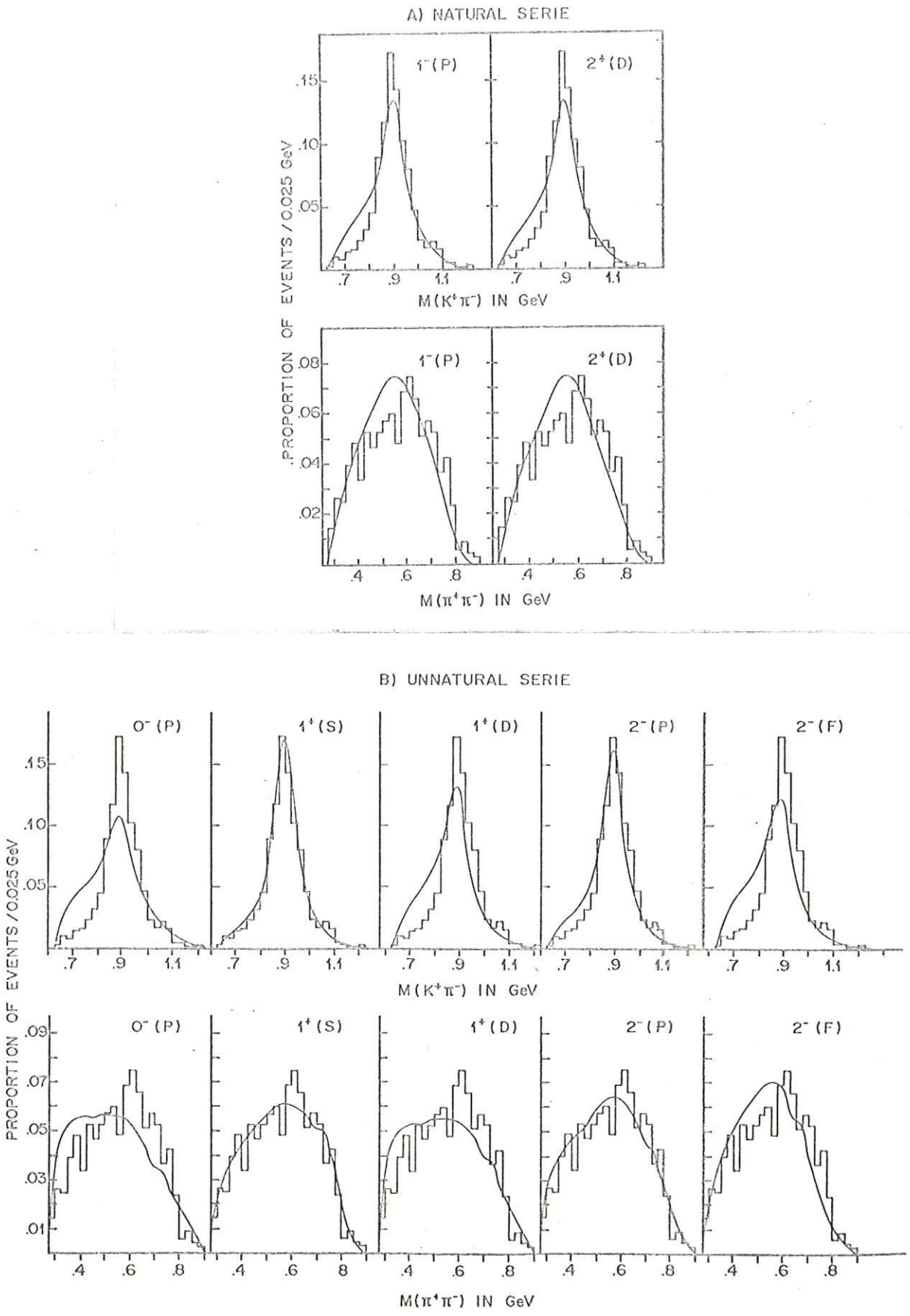

Fig. 4 : Fits to the Dalitz plot projections for the different hypotheses of the natural serie (A) and the unnatural serie (B)

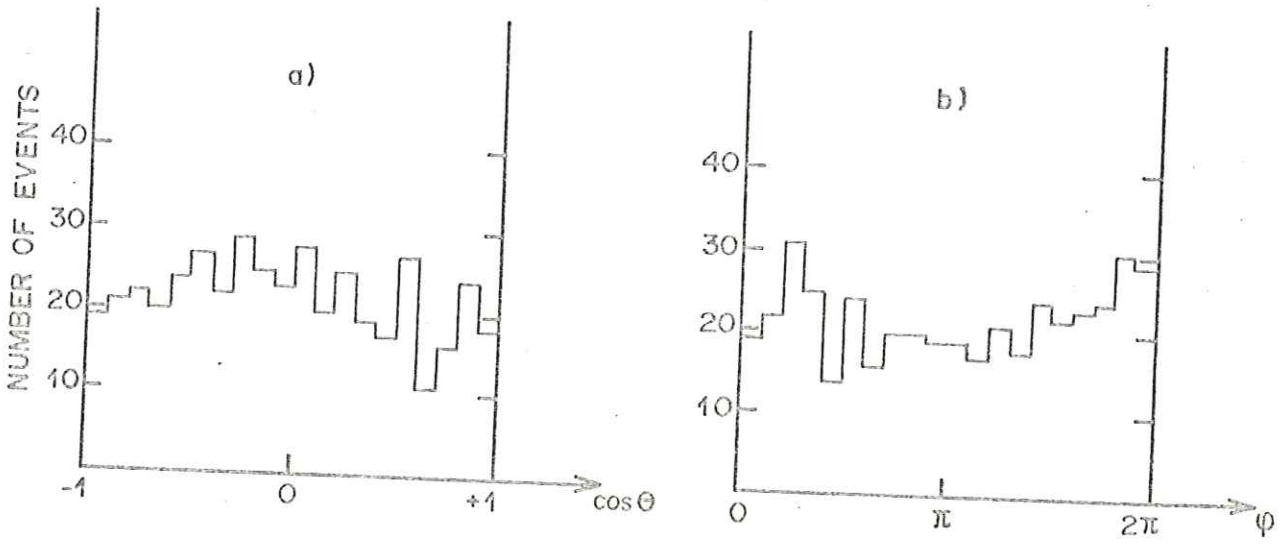

Fig. 5 : Polar (a) and azimuthal (b) emission angles of the K^* in the Q^+ center of mass system of the $Q^+ \to K^*\pi$ events. A pure $1^+(S)$ state would give isotropic distributions

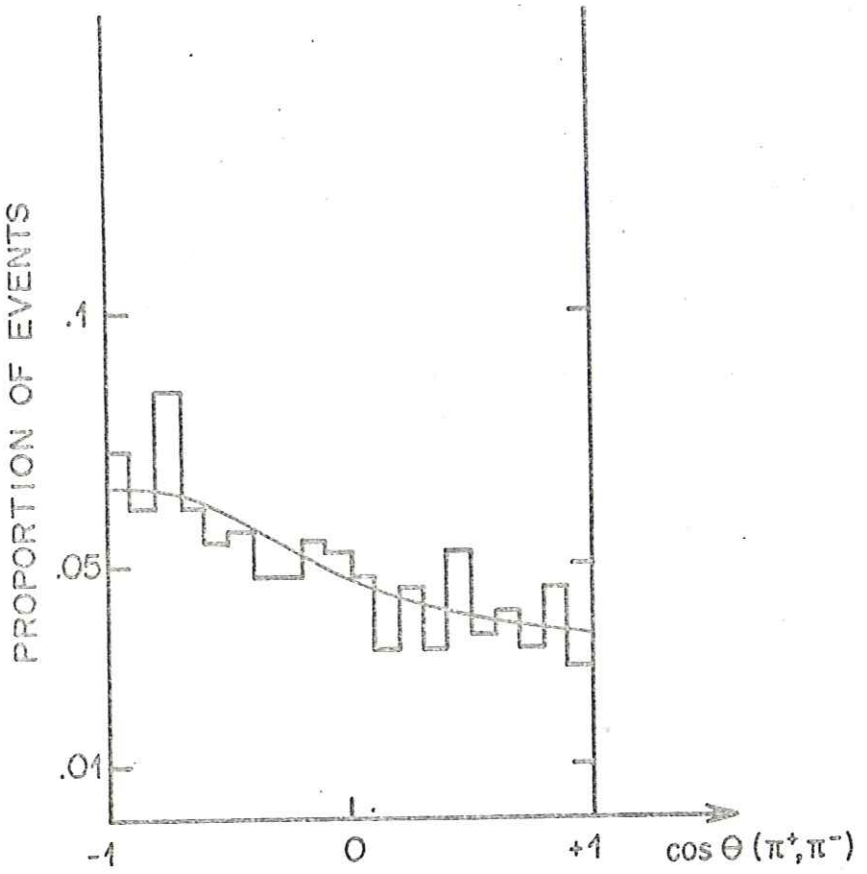

Fig. 6 : Distribution of the cosine of the angle between π^+ and π^- evaluated in the K^* center of mass system, for the $Q^+ \to K^* \pi$ events. The curve corresponds to the fit of the Dalitz plot density to the $1^+(S)$ hypothesis

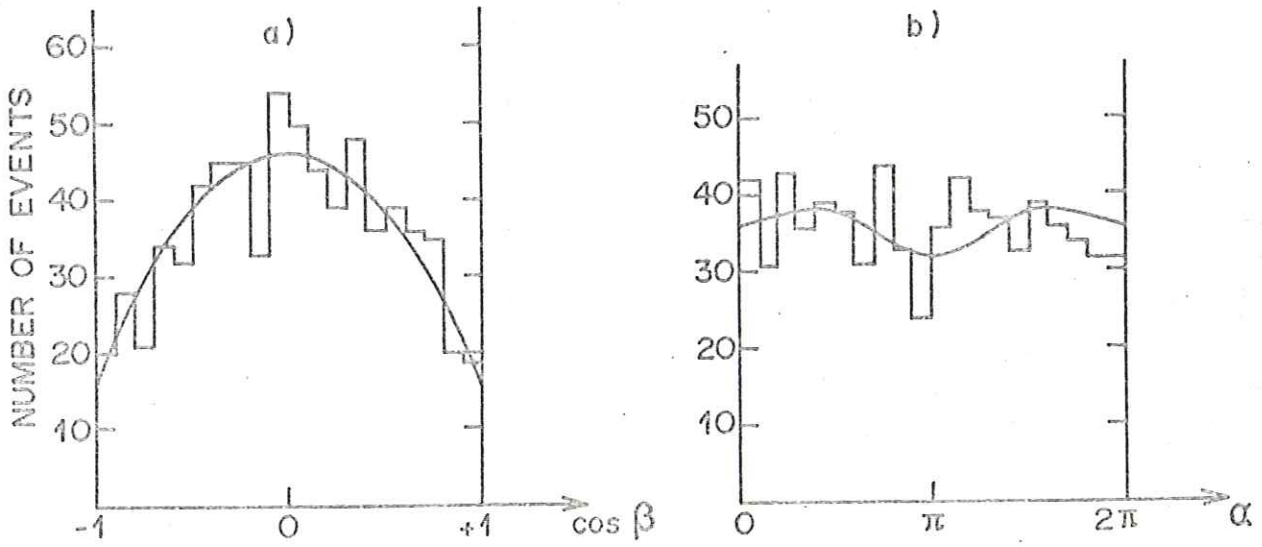

Fig. 7 : Polar (a) and azimuthal (b) distributions of the direction of the normal to the Q^+ decay plane. The angles are evaluated for the τ frame in the Q^+ center of mass system. The curve corresponds to the $1^+(S)$ fitted distribution (see formula (19)).

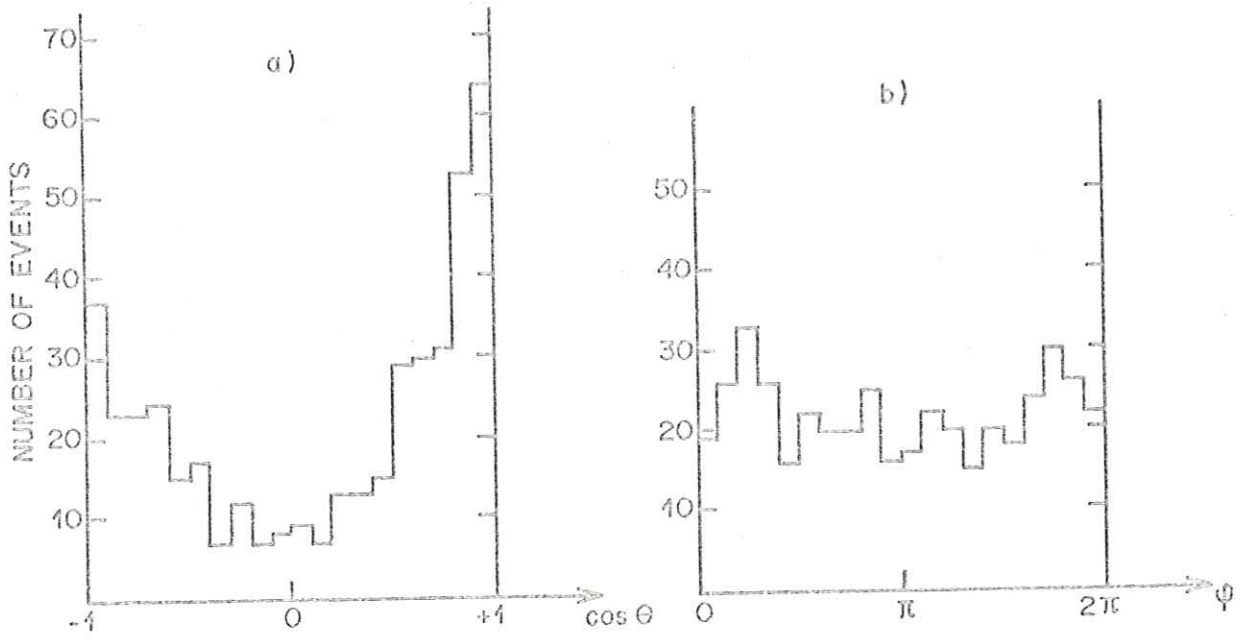

Fig. 8 : Alignment (a) and azimuthal (b) angles for the K^* ($Q^+ \to K^* \pi^+$ events) in the K^* center of mass system